arXiv:1303.3459v1 [cond-mat.quant-gas] 14 Mar 2013

A non-equilibrium model of photon condensation

Peter Kirton and Jonathan Keeling
SUPA, School of Physics and Astronomy, University of St Andrews, KY16 9SS, United Kingdom
(Dated: March 15, 2013)

We develop a non-equilibrium quantum model of Bose-Einstein condensation and lasing of photons in a dye filled microcavity. We examine in detail the nature of the thermalization process induced by absorption and emission of photons by the dye molecules, and investigate when the photons are able to reach a thermal equilibrium Bose-Einstein distribution. At low temperatures, or large cavity losses, the absorption and emission rates are too small to allow the photons to reach thermal equilibrium and the behavior becomes more like that of a conventional laser.

Bose-Einstein condensation (BEC) has been observed in a wide variety of systems, from ultra-cold atomic gases [1, 2] to quasi-particles in solid state systems such as polaritons [3–6], excitons [7] and magnons [8]. Recently experiments have also shown convincing evidence of a Bose-Einstein distribution, and macroscopic occupation for a gas of photons confined in a dye-filled optical microcavity [9–12]. In these experiments, the thermal equilibrium distribution of photons arises because of phonon-dressing of the absorption and emission by the dye molecules, and the rapid thermalisation of vibrational modes of the dye molecules by their collisions with the solvent. This leads to the accumulation of low energy photons, closely following a Bose-Einstein distribution, as is clearly seen experimentally [10].

Such a system is very closely related to a dye laser [13], but differs in the near-thermal emission that is observed below and near threshold. In the context of polariton condensation [3–6] there has been much debate [14, 15] about the extent to which the lack of thermal equilibrium in polariton experiments means the system should be called a condensate or a laser. However calculations for polaritons using various methods, from quantum kinetics [16, 17] to Schwinger-Keldysh path integrals [18], have shown that there is a relatively smooth crossover between behavior typical of a laser, and that typical of an equilibrium condensate.

Both lasers and condensates involve a spontaneous phase symmetry breaking, and a transition to a macroscopically occupied quantum state, and so, as has long been recognized [19], they share many features. However, recent experiments on polariton and photon condensates also show what important differences arise, for example, showing how thermalisation may lead to lasing without inversion. In the context of polariton condensates, this is closely connected with the possibility of lasing in strong coupling [18]. The coupling in the photon condensate, however, remains weak, and the thermal Bose-Einstein distribution seen in this system can be understood as arising from the combination of asymmetry between absorption and emission and the re-trapping of fluorescence. A theoretical description of how asymmetric absorption and emission could be engineered in a circuit QED setting was recently discussed by Marthaler *et al.* [20]. In this Letter, we extend such an approach to understand lasing without inversion, thermalisation, and the limits in which equilibrium behavior is seen for the dye-filled optical cavity. We find that over a range of parameters (including those used in the experiments) the system shows BEC-like behavior. However, significant deviations from this occur if the cavity losses are made larger, and a crossover toward more standard lasing behavior is observed.

Some theoretical work has attempted to produce models of this system from the point of view of *equilibrium* statistical mechanics [21, 22], while other work has examined the emergence of phase coherence in a BEC where particles interact through an intermediate medium [23]. We aim instead to provide a general *non-equilibrium* framework for understanding the steady state properties of the photons, taking into account the pump and decay processes. This allows one to understand how these compete with thermalization process, and control when the system behaves like a laser or like a condensate.

A schematic diagram of our model is shown in Fig. 1. This consists of a photon modes, with creation operators $a_m^\dagger$, confined in the optical cavity coupled to a single electronic transition of the dye molecules. Dye molecules are represented as two-level systems, written as Pauli matrices σ_i with splitting Δ between ground and excited levels. These levels are dressed by ladders of rovibrational states, which can be thought of as an on-site phonon [13], described by operators $b_i, b_i^\dagger$. The level scheme is shown in the insert to Fig. 1. The Hamiltonian is thus:

$$H = \sum_m \omega_m a_m^\dagger a_m + \sum_i \frac{\Delta}{2}\sigma_i^z + \Omega\left(b_i^\dagger b_i + \sqrt{S}\sigma_i^z(b_i + b_i^\dagger)\right) + g\sum_{m,i}\left(a_m\sigma_i^+ + a_m^\dagger\sigma_i^-\right). \quad (1)$$

As in the experiment [10], we consider photon modes in a two-dimensional harmonic potential (arising from the curvature of the mirrors). We therefore take regularly spaced oscillator levels $\omega_m = \omega_0 + m\epsilon$, having a degeneracy g_m given by $g_m = m + 1$. The lowest frequency ω_0 is the "cavity cutoff". In the following we quote frequencies relative to the molecular splitting Δ and thus introduce $\delta_m = \omega_m - \Delta$. If in equilibrium, Bose condensation would lead to a macroscopic occupation of the

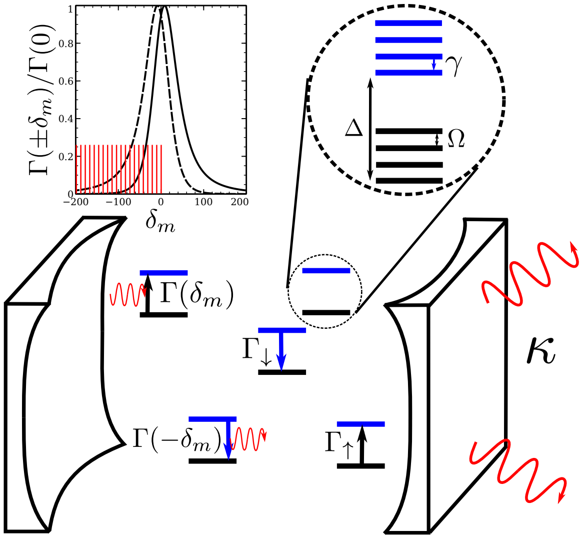

FIG. 1. (Color online) Cartoon of the system showing the decay processes included in Eq. (2). The zoomed in view shows the energy level structure of the dye molecules. The graph shows the characteristic behavior of the emission rate, $\Gamma(-\delta_m)$ (dashed line) and the absorption rate, $\Gamma(\delta_m)$ (solid line) described in the main text. The vertical (red) lines show the typical spacing of the photon modes confined in the cavity.

lowest mode. As discussed later, the extent of thermalisation is affected by the detuning of the cavity cutoff, δ_0. Since the light-matter coupling is small compared to optical frequencies, we assume a Jaynes-Cummings coupling, with frequency independent coupling strength g. The vibrational mode spacing is Ω, and the interaction between electronic and vibrational states is given by the dimensionless Huang-Rhys parameter S, which characterizes the difference in phonon displacement between the ground and excited states. The parameter values we use, corresponding to the experiment [10], are given in figure captions.

To model the open system, we must add additional loss processes and external pumping. We include the loss of cavity photons with rate κ, assumed independent of the photon frequency, and a rate $\Gamma_\downarrow$ describing fluorescence of the dye molecules into non-cavity modes. To balance these losses we include a pumping term with rate $\Gamma_\uparrow$. These processes may all be described by standard Markovian Lindblad terms, as there is no significant thermal occupation of relevant photon modes outside the cavity. The localized vibrational modes also undergo incoherent relaxation, due to scattering off of the solvent molecules. This is modeled as a relaxation rate γ toward a thermal equilibrium state at temperature T. These processes cannot be described by Markovian loss rates, as this cannot describe thermalisation of the radiation [24, 25]. Below we describe an alternate approach to include these processes. For a good cavity, where equilibrium may be reached, $1/\kappa$ is the longest timescale.

If the coupling to phonons, S, is reasonably strong, then multiphonon effects will be important in describing the thermalisation processes. These can be captured by making a polaron transformation $H \to U^\dagger H U$ where $U = \exp[\sum_i \sqrt{S}\sigma_i^z(b_i - b_i^\dagger)]$. Since the coupling of molecules to the optical modes is weak, we then treat the dynamics perturbatively in g while keeping all orders of S. Working in the interaction picture, and expanding the Liouville equation to second order in g, one may then trace out the degrees of freedom associated with the vibrational mode and its damping. The resulting equation of motion then contains Lindblad terms which cause simultaneous transitions in both the photon field and the dressed molecule [20]. These processes then describe the emission (absorption) of photons into (from) the cavity, as shown schematically in Fig. 1. Including all processes, the resulting master equation for the photon-molecule system is:

$$\dot{\rho} = -i[H_0, \rho] - \sum_{i,m} \left\{ \frac{\kappa}{2}\mathcal{L}[a_m] + \frac{\Gamma_\uparrow}{2}\mathcal{L}[\sigma_i^+] + \frac{\Gamma_\downarrow}{2}\mathcal{L}[\sigma_i^-] + \frac{\Gamma(-\delta_m)}{2}\mathcal{L}[a_m^\dagger \sigma_i^-] + \frac{\Gamma(\delta_m)}{2}\mathcal{L}[a_m \sigma_i^+] \right\} \rho. \quad (2)$$

Here the system Hamiltonian is $H_0 = \sum_m \delta_m a_m^\dagger a_m$ and $\mathcal{L}[X]\rho = \{X^\dagger X, \rho\} - 2X\rho X^\dagger$ is the usual Lindblad term. The phonon assisted emission and absorption rates are given by the function [20],

$$\Gamma(\omega) = g^2 \int_{-\infty}^{\infty} dt f(t) \mathrm{e}^{-(\Gamma_\uparrow + \Gamma_\downarrow)|t|/2} \mathrm{e}^{-i\omega t}, \quad (3)$$

evaluated at the detuning of the relevant photon mode. Here $f(t)$ is a correlation function of polaron operators [20, 26, 27] given by,

$$f(t) = \exp\left[-\frac{2S\gamma}{\pi} \int_{-\infty}^{\infty} d\nu \frac{2\sin^2\frac{\nu t}{2}\coth\frac{\beta\nu}{2} + i\sin\nu t}{(\Omega - \nu)^2 + \frac{\gamma^2}{4}} \right]. \quad (4)$$

An illustration of these rates, as a function of detuning, is shown in Fig. 1. We note that for frequencies where the rates $\Gamma_\uparrow, \Gamma_\downarrow$ can be ignored in Eq. (3), the vibration induced emission and absorption rates are related by a Boltzmann factor $\Gamma(\delta) = \mathrm{e}^{-\beta\delta}\Gamma(-\delta)$[28] with β corresponding to the phonon (solvent) temperature, thus satisfying the Kennard-Stepanov relation between absorption and emission rates [29]. At large frequencies $\Gamma(\omega)$ ceases to obey this relation because the incoherent pumping process corresponds to coupling to a white noise (i.e. infinite temperature) bath [25].

Marthaler *et al.* [20] considered this kind of Master equation as a route to lasing without inversion in circuit QED. The same mechanism they proposed also applies for the photon condensate, allowing coherent emission far below inversion: if $\Gamma(-\delta_m) > \Gamma(\delta_m)$ then the asymmetry in emission and absorption induced by thermalisation with the phonons allows net gain without inversion. For lasing to occur significantly below the inversion point we require $\delta_0 \ll -T$ so that the asymmetry of the absorption and emission rates is sufficiently large. As we will discuss below, the same conditions lead to thermalized lasing, as long as the relevant emission rates $\Gamma(-\delta_m)$ are large enough to overcome the losses from the cavity.

We can use the master equation, Eq. (2), to derive a semi-classical rate equation for the population of each photon mode which, after adiabatically eliminating the N molecular degrees of freedom, is:

$$\frac{\partial n_m}{\partial t} = -\kappa n_m + N \frac{\Gamma(-\delta_m)(n_m+1)\tilde{\Gamma}_\uparrow - \Gamma(\delta_m) n_m \tilde{\Gamma}_\downarrow}{\tilde{\Gamma}_\uparrow + \tilde{\Gamma}_\downarrow}, \tag{5}$$

where we define $\tilde{\Gamma}_\uparrow = \Gamma_\uparrow + \sum_m g_m \Gamma(\delta_m) n_m$ and $\tilde{\Gamma}_\downarrow = \Gamma_\downarrow + \sum_m g_m \Gamma(-\delta_m)(n_m+1)$. We can then use the steady state of this expression in combination with the rates from Eq. (3) to calculate the photon population in each mode, $g_m n_m$. Note that the $n_m + 1$ term in the emission process corresponds to the trapping of spontaneous fluorescence from the dye. Along with the Kennard-Stepanov relation discussed above, this means that in the equilibrium limit $\kappa, \Gamma_\uparrow, \Gamma_\downarrow \to 0$, but $\Gamma_\uparrow/\Gamma_\downarrow$ finite, the below threshold solution to this equation is simply an equilibrium Bose-Einstein distribution with an effective chemical potential given by $\mu_{\text{eff}} = T \ln(\Gamma_\uparrow/\Gamma_\downarrow)$ which condenses when $\mu_{\text{eff}} = \delta_0$.

In Fig. 2(a) we present results for parameter values (given in the caption) typical of those in the experiments of Refs. [9–11]. We fit Bose-Einstein distributions to the data by tuning the chemical potential so that the tail matches the numerical results. At pump powers far below threshold the occupation of the modes is, to a very good approximation, given by a Boltzmann distribution (in this limit the $\mu_{\text{eff}} \ll \delta_0$ so the distribution is classical). For pump strengths above the condensation threshold there is a macroscopic occupation of the lowest energy mode. The chemical potential approaches this mode, producing a condensate. If the pump is increased even further beyond this point (so that more modes are above threshold) the only effect is that the occupation of the lowest energy mode increases further, the shape of the tail does not change.

The profile changes dramatically when the cavity loss rate is increased, as shown in Fig. 2(b). In this case the losses for the lowest energy modes exceeds the gain, controlled by the rate $\Gamma(-\delta_0)$. The loss dominates these modes, thus preventing the low energy modes from reaching thermal equilibrium. As can be clearly seen in the figure, the modes with higher energy (i.e. $\delta_m \simeq 0$) still match the Bose-Einstein distributions well. At sufficiently strong pumping there is a threshold (at much higher power than would be required if in thermal equilibrium) above which we find a macroscopic peak appears in an excited mode of the cavity. The mode that condenses is determined by the lowest mode such that $\Gamma(-\delta_m)$ is large enough to overcome the losses. For the parameters of Fig. 2(b) the thermalisation still plays a role in the rates of emission and absorption, so that it is not the mode with peak emission rate (near $\delta_m = 0$) which condenses. However, at yet higher decay rates, the behavior crosses over toward such "standard" laser behavior, and all thermal properties are lost. Similarly, as $T \to 0$ the emission and absorption spectra become a narrow Lorentzian peak at $\delta_m = 0$, and condensation moves to the center of the gain peak.

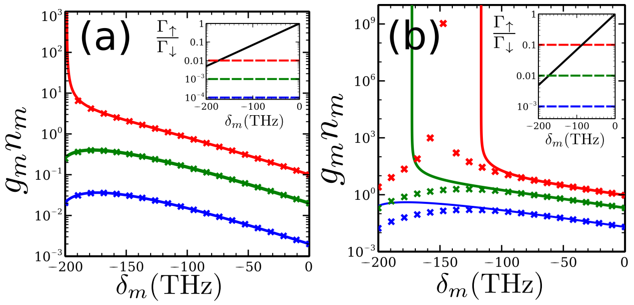

FIG. 2. (Color online) Mode populations $g_m n_m$ vs detuning δ_m for various pump strengths. Stars are results of the non-equilibrium model, and lines show Bose-Einstein distributions fitted to the tail of the numerical results. Insets show the pump powers, $\Gamma_\uparrow/\Gamma_\downarrow = e^{\beta\mu_{\text{eff}}}$, (dashed lines) compared to the ratio $\Gamma(-\delta_m)/\Gamma(\delta_m) \simeq e^{\beta\delta_m}$ (solid, black line) which gives a good approximation to the threshold. Panel (a) corresponds to experimental losses, $\kappa = 10$MHz. Panel (b) shows $\kappa = 5$GHz where losses prevent thermalisation. Other parameters are: $\gamma = 100$THz, $\Gamma_\downarrow = 1$GHz, $S = 0.5$, $\Omega = 1$THz, $N = 10^{11}$, $g = 0.1$GHz, $T = 300$K, $\delta_0 = -200$THz and the mode spacing $\epsilon = 10$THz.

Since the origin of the destruction of thermalization is the competition between loss κ and emission rate $\Gamma(-\delta_0)$, it is also clear that lowering the cavity cutoff (making δ_0 more negative) has a similar effect. Equilibrium behavior can only be seen when the cavity cutoff is sufficiently close to the molecular frequency, which ensures that $\Gamma(-\delta_0)$ is sufficiently large.

In order to explore the degree of thermalisation as a function of temperature and loss rates, we next consider the behavior at threshold. We examine two different aspects; the threshold pump power (a measure typical when considering lasing), and the total photon density at threshold (a measure typical for an equilibrium condensation transition). Fig. 3(a) shows the total number of photons in the cavity, $N_{\text{tot}} = \sum_m g_m n_m$, as a function of the pump rate, $\Gamma_\uparrow$, at various temperatures. As expected, increasing the temperature of the phonons reduces the asymmetry between $\Gamma(\delta_m)$ and $\Gamma(-\delta_m)$, and thus both the pump power and total density at threshold increase. To explore temperature dependence we identify the threshold as the lowest pump power where $\max(n_m) > 2$ — note that this maximally occupied mode

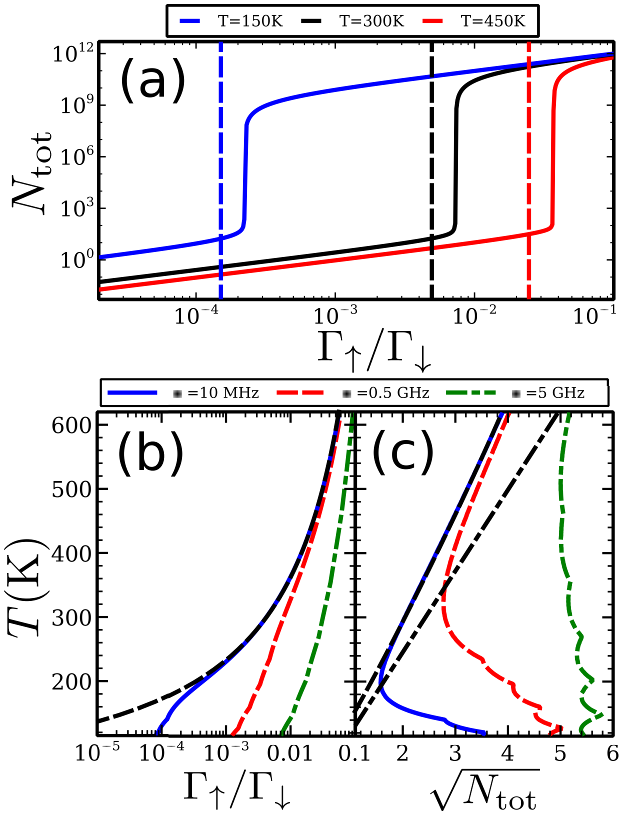

FIG. 3. (Color online) Panel (a): total number of photons in the cavity $N_{\rm tot}$ vs pump power. The dashed vertical lines show the threshold (defined by $\max(n_m) = 2$). Panel (b): threshold pump power vs temperature, for various cavity loss rates as indicated. The dashed (black) lines show the same threshold calculated for the equilibrium theory. Panel (c): population $N_{\rm tot}$ at threshold vs temperature for the same loss rates shown in (b). The dashed (black) line is the equilibrium prediction of critical density accounting for finite mode spacing; the dash-dot (black) line is the equilibrium continuum limit discussed in the text. All other parameters are the same as in Fig. 2.

is not necessarily the lowest energy mode.

Figure 3(b) shows the threshold pump power vs temperature at various cavity loss rates. As T decreases the absorption and emission rates at a given detuning δ_m decrease. At low temperatures this again means that the loss rates exceed the gain for the lowest frequencies, and thermalisation breaks down. The temperature at which this happens increases with increasing κ. For the strongly lossy case, shown by the dot-dashed (green) curve [corresponding to the κ used in in Fig. 2(b)] then the threshold is shifted across the whole temperature range shown. In the high temperature limit the emission and absorption rates are symmetric, so the threshold pump strength eventually becomes that required to reach inversion.

A more common description of the "threshold" for equilibrium Bose condensation is the temperature dependent critical number of particles, i.e. the total number of photons in the cavity at threshold. For particles confined in 2D one expects $N_{\rm tot} \propto T^2$ [30]. In Fig. 3(c) we plot this critical number for the same values of κ as used in Fig. 3(b). Along side these results we also plot, as the dashed (black) curve the same quantity calculated assuming the mode profile is Bose-Einstein distributed with a chemical potential, $\mu = \delta_0 - T\ln(3/2)$, this ensures that the lowest energy mode has an occupation of 2. For comparison we also show the simple analytic result in the continuum limit [30], $N_{\rm tot} = \pi^2 T^2/6\epsilon^2$ where ϵ is the mode spacing. This differs from the discrete results due to the different definitions of threshold, the discrete mode spacing, and the effect of very high energy photon modes, which are neglected in the numerical calculations.

For small cavity losses we see that for temperatures above ~ 200K the agreement between the discrete Bose distribution and the numerics is very close. Below this temperature, the mode which condensed is no longer the lowest energy mode, and condensation requires stronger pumping. This leads to an increase in the critical number of photons at low temperatures. As κ is increased we again see that the temperature above which the results match a Bose distribution increases. There are also notable oscillations in the critical number at low temperatures. These occur as the mode which gains a macroscopic population jumps to higher and higher energy.

In conclusion we have presented a simple non-equilibrium model which accurately describes the steady state properties of the dye filled cavity systems used to observe BEC of photons. We found that, for relevant parameters, our model accurately predicts the onset of BEC and the equilibrium dependence of pump power and critical photon number on temperature. If the losses from the cavity are increased, the temperature reduced, or the detuning increased compared to those used in the experiment, then a crossover occurs toward behavior more typical of a laser, and thermalisation is suppressed. These results show that, as for polariton condensation [18], a smooth crossover between typical laser behavior and equilibrium condensation can arise. In contrast to the polariton case, the process described here involves a thermalized stimulated emission of radiation, rather than stimulated scattering between different photon or polariton modes [23]. Future studies of the time dynamics of how coherence arises, and the thermal distribution emerges following the switch-on of the pump can help to clarify this behavior, and can be predicted using the model presented here.

The authors would like to thank M. Weitz and J. Klaers for useful discussions and acknowledge financial support from EPSRC program "TOPNES" (EP/I031014/1) and EPSRC (EP/G004714/2)

---

[1] M. H. Anderson, J. R. Ensher, M. R. Matthews, C. E. Wieman, and E. A. Cornell, Science **269**, 198 (1995).

[2] K. B. Davies, M.-O. Mewes, M. R. Andrews, N. J. van Druten, D. S. Durfee, D. M. Kurn, and W. Ketterle, Phys. Rev. Lett. **75**, 3969 (1995).

[3] J. Kasprzak, M. Richard, S. Kundermann, A. Baas, P. Jeambrun, J. M. J. Keeling, F. M. Marchetti, M. H. Szymaska, R. André, J. L. Staehli, V. Savona, P. B. Littlewood, B. Deveaud, and L. S. Dang, Nature **443**, 409 (2006).

[4] R. Balili, V. Hartwell, D. Snoke, L. Pfeiffer, and K. West, Science **316**, 1007 (2007).

[5] H. Deng, H. Haug, and Y. Yamamoto, Rev. Mod. Phys. **82**, 1489 (2010).

[6] I. Carusotto and C. Ciuti, Rev. Mod. Phys. **85**, 299 (2013).

[7] A. A. High, J. R. Leonard, A. T. Hammack, M. M. Fogler, L. V. Butov, A. V. Kavokin, K. L. Campman, and A. Gossard, Nature **483**, 584 (2012).

[8] S. O. Demokritov, V. E. Demidov, O. Dzyapko, G. a. Melkov, a. a. Serga, B. Hillebrands, and a. N. Slavin, Nature **443**, 430 (2006).

[9] J. Klaers, F. Vewinger, and M. Weitz, Nature Physics **6**, 512 (2010).

[10] J. Klaers, J. Schmitt, F. Vewinger, and M. Weitz, Nature **468**, 545 (2010).

[11] J. Klaers, J. Schmitt, T. Damm, F. Vewinger, and M. Weitz, Applied Physics B **105**, 17 (2011).

[12] J. Schmitt, T. Damm, F. Vewinger, M. Weitz, and J. Klaers, New J. Phys. **14**, 075019 (2012).

[13] F. P. Schäfer, in *Dye Lasers*, edited by F. P. Schäfer (Springer-Verlag, 1990) 3rd ed.

[14] L. V. Butov, Nature **447**, 540 (2007).

[15] D. Snoke, Nat. Phys. **4**, 673 (2008).

[16] T. D. Doan, H. Thien Cao, D. B. Tran Thoai, and H. Haug, Phys. Rev. B **72**, 85301 (2005); Phys. Rev. B **74**, 115316 (2006); Phys. Rev. B **78**, 205306 (2008).

[17] J. Kasprzak, D. Solnyshkov, R. André, L. Dang, and G. Malpuech, Phys. Rev. Lett. **101**, 146404 (2008).

[18] M. H. Szymanska, J. Keeling, and P. B. Littlewood, Phys. Rev. Lett **96**, 230602 (2006); in *Quantum Gases: Finite Temperature and Non-equilibrium Dynamics*, edited by N. P. Proukakis, S. Gardiner, M. J. Davis, and M. H. Szymanska (Imperial College Press, London, 2013).

[19] H. Haken, Rev. Mod. Phys. **47**, 67 (1975).

[20] M. Marthaler, Y. Utsumi, D. Golubev, A. Shnirman, and G. Schön, Phys. Rev. Lett. **107**, 093901 (2011).

[21] J. Klaers, J. Schmitt, T. Damm, F. Vewinger, and M. Weitz, Phys. Rev. Lett. **108**, 160403 (2012).

[22] W. Fan, M. Yin, and Z. Cheng, (2013), arXiv:1301.7136.

[23] D. W. Snoke and S. M. Girvin, J. Low. Temp. Phys. **171** (2013).

[24] G. Ford and R. O'Connell, Phys. Rev. Lett. **77**, 798 (1996).

[25] M. Lax, Optics Commun. **179**, 463 (2000).

[26] I. Wilson-Rae and A. Imamolu, Phys. Rev. B **65**, 235311 (2002).

[27] D. McCutcheon and A. Nazir, Phys. Rev. B **83**, 165101 (2011).

[28] This expression arises due to a Kubo-Martin-Schwinger relation [31] between the time domain rates $f(t) = f(-t - i\beta)$.

[29] E. H. Kennard, Phys. Rev. **11**, 29 (1918); Phys. Rev. **28**, 672 (1926); B. I. Stepanov, Dokl. Akad. Nauk SSR **112**, 839 (1957).

[30] L. P. Pitaevskii and S. Stringari, *Bose-Einstein Condensation* (Clarendon Press, Oxford, 2003).

[31] R. Kubo, J. Phys. Soc. Jpn. **12**, 570 (1957); P. Martin and J. Schwinger, Phys. Rev. **115**, 1342 (1959).